No systematic effects of sampling direction on climate-growth relationships in a large-scale, multi-species tree-ring data set

Urs Gut[1,2]*, Mátyás Árvai[3], Szymon Bijak[4], J. Julio Camarero[5], Anna Cedro[6], Roberto Cruz-García[7], Balázs Garamszegi[8], Andrew Hacket-Pain[9], Andrea Hevia[10], Weiwei Huang[11,12], Miriam Isaac-Renton[13], Ryszard J. Kaczka[14], Marko Kazimirović[15], Wojciech Kędziora[16], Zoltán Kern[17], Marcin Klisz[18], Tomáš Kolář[19,20], Michael Körner[21], Veronica Kuznetsova[22], David Montwé[23], Any Mary Petritan[24], Ion Catalin Petritan[25], Lenka Plavcová[26], Romy Rehschuh[27], Eva Rocha[28], Michal Rybníček[19,20], Raúl Sánchez-Salguero[29], Jens Schröder[21], Niels Schwab[30], Branko Stajić[15], Robert Tomusiak[4], Martin Wilmking[7], Ute Sass-Klaassen[31], and Allan Buras[31,32]

[1]Institut für Archäologie, Fachbereich Prähistorische Archäologie, University of Zurich, Zurich, 8006, Switzerland, [2]Department of Environmental System Science, Institute of Terrestrial Ecosystems, Forest Ecology, ETH Zurich, 8092, Zurich, Switzerland, [3]Institute for Soil Sciences and Agricultural Chemistry, MTA Centre for Agricultural Research, 1022, Budapest, Hungary, [4]Dendrometry and Forest Productivity, Warsaw University of Life Sciences – SGGW, 02-776, Warszawa, Poland, [5]Pyrenean Institute of Ecology, Spanish Research Council, CSIC, 50059, Zaragoza, Spain, [6]Department of Geosciences, Szczecin University, 70–383, Szczecin, Poland, [7]Landscape Ecology and Ecosystem Dynamics, Greifswald University, 17487, Greifswald, Germany, [8]Forest Research Institute, National Agricultural Research and Innovation Centre, 9600, Sárvár, Hungary, [9]Department of Geography and Planning, University of Liverpool, L69 7ZT, Liverpool, United Kingdom, [10]Dept. de Ciencias Agroforestales, Escuela Técnica

Superior de Ingeniería, Universidad de Huelva, 21819, La Rábida, Spain, [11]Bamboo Research Institute, Nanjing Forestry University, 210037, Nanjing, China, [12]Department of Geosciences and Natural Resource Management, University of Copenhagen, 1958, Frederiksberg C, Denmark, [13]Canadian Wood Fibre Centre, Natural Resources Canada, V8Z 1M5, Victoria, Canada, [14]Faculty of Earth Sciences, University of Silesia, 41-200, Sosnowiec, Poland, [15]Faculty of Forestry, University of Belgrade, 11000, Belgrade, Serbia, [16]Forest Management Planning, Warsaw University of Life Sciences – SGGW, 02-776, Warszawa, Poland, [17]Institute for Geological and Geochemical Research, Research Centre for Astronomy and Earth Sciences, MTA, 1112, Budapest, Hungary, [18]Department of Silviculture and Forest Tree Genetics, Forest Research Institute, 05-090, Raszyn, Poland, [19]Department of Wood Science, Mendel University, 613 00, Brno, Czech Republic, [20]Global Change Research Institute of the Czech Academy of Sciences, 603 00, Brno, Czech Republic, [21]Faculty of Forest and Environment, Eberswalde University for Sustainable Development, 16225, Eberswalde, Germany, [22]Glaciology, Institute of Geography, Russian Academy of Sciences, 119017, Moscow, Russia, [23]Centre for Forest Biology, University of Victoria, V8W 2Y2, Victoria, Canada, [24]Forest Ecology, National Institute for Research and Development in Forestry “Marin Drăcea”, 500040, Brasov, Romania, [25]Sylviculture and Forest Engineering, University of Transylvania, 500123, Brasov, Romania, [26]Department of Biology, University of Hradec Králové, 500 03, Hradec Králové, Czech Republic, [27]Institute of Meteorology and Climate Research - Atmospheric Environmental Research (IMK-IFU), Karlsruhe Institute of Technology (KIT), 82467, Garmisch-Partenkirchen, Germany, [28]Department of Physical Geography, Stockholm University, 106 91, Stockholm,

Sweden, [29]Dept. de Sistemas Físicos, Químicos y Naturales, Universidad Pablo de Olavide, 41013, Sevilla, Spain, [30]Physical Geography, Center for Earth System Research and Sustainability (CEN), Universität Hamburg, 20146, Hamburg, Germany, [31]Forest Ecology and Forest Management, Wageningen University and Research, 6708 PB, Wageningen, Netherlands, [32]Land Surface-Atmosphere Interactions, Technische Universität München, 85354, Freising, Germany.

*Corresponding author. *Address*: Universität Zürich, Institut für Archäologie, Fachbereich Prähistorische Archäologie, Karl Schmid-Strasse 4, 8006 Zürich, Switzerland. *E-mail address*: u.gut@posteo.de (U. Gut).

Highlights

- Direction-specific climate signals were investigated using cores from 22 sites.
- International (10 countries), multi-species (8 species) tree-ring network.
- Signal strength, climate correlations and Principal Component Gradient Analysis.
- No systematic directional bias introduced in high-pass filtered ring-width series.
- Directional effects negligible for sites within forests in flat terrain.

Abstract

Ring-width series are important for diverse fields of research such as the study of past climate, forest ecology, forest genetics, and the determination of origin (dendro-provenancing) or dating of archeological objects. Recent research suggests diverging climate-growth relationships in tree-rings due to the cardinal direction of extracting the

tree cores (i.e. direction-specific effect). This presents an understudied source of bias that potentially affects many data sets in tree-ring research.

In this study, we investigated possible direction-specific growth variability based on an international (10 countries), multi-species (8 species) tree-ring width network encompassing 22 sites. To estimate the effect of direction-specific growth variability on climate-growth relationships, we applied a combination of three methods: An analysis of signal strength differences, a Principal Component Gradient Analysis and a test on the direction-specific differences in correlations between indexed ring-widths series and climate variables.

We found no evidence for systematic direction-specific effects on tree radial growth variability in high-pass filtered ring-width series. In addition, direction-specific growth showed only marginal effects on climate-growth correlations. These findings therefore indicate that there is no consistent bias caused by coring direction in data sets used for diverse dendrochronological applications on relatively mesic sites within forests in flat terrain, as were studied here. However, in extremely dry, warm or cold environments, or on steep slopes, and for different life-forms such as shrubs, further research is advisable.

Keywords

Tree-rings; Directional Growth; Climate Signal; Dendro-provenancing; Principal Component Gradient Analysis; Correlation Analysis

1 Introduction

Tree-ring records provide valuable data for various scientific disciplines. For example, tree-rings are used in paleoclimatology, as a proxy for reconstructing past climate (Hughes et al., 2011); in ecology, for investigating stand dynamics (Amoroso et al., 2017; Schweingruber, 1996); and in history and archaeology, for dating of artifacts and wooden construction elements as well as for analyzing past usage of timber resources (Bleicher and Harb, 2015; Eissing and Dittmar, 2011).

Tree growth is dependent on environmental, climatic and biotic factors (Cook and Kairiukstis, 1990). Through careful sampling design and selection of appropriate statistical methods, certain growth signals in ring-width series may be selectively enhanced (Fritts, 1976; Sullivan and Csank, 2016). In dendro-climatology, for example, the climatically-related environmental signal is of primary importance. Thus, sampling is commonly conducted on trees growing at the species distributional margins where the desired climatic factor is assumed to limit tree-growth, for example, growing-season temperature in cold environments or precipitation in dry environments (Fritts, 1976; Klesse et al., 2018). In addition, statistical detrending is used to remove the age-size-related trend (Cook and Kairiukstis, 1990; Melvin and Briffa, 2008; Peters et al., 2015). To amplify growth signals shared by a tree population and averaging out individual-specific noise, mean site tree-ring width chronologies are calculated (Cook and Kairiukstis, 1990). Often, this approach leads to absolutely higher correlations between climate variables and master chronologies in comparison to climate correlations at the individual tree level (Carrer, 2011; Galván et al., 2014).

A recent study by Fang et al. (2015) suggested the potential for inadvertent sampling bias due to commonly-used sampling procedures such as coring individual trees from random or ‘ad hoc’ radial directions. Their results provided evidence for diverging climate-growth relationships between ring-width series from the same tree cored from different cardinal directions for *Pinus tabuliformis* Carrière and *Picea purpurea* Mast. Thus, mean site chronologies might enhance an already biased climate signal if they were based on a low replication and/or samples that were taken with a systematic preference for an azimuth coring direction. For example, most standard sampling protocols recommend extracting tree cores at positions where the trunk is perpendicular to the slope and parallel to the contour line (Speer, 2010; Yang et al., 2018). Such sampling protocols seek to avoid reaction wood. At the same time, certain cardinal directions of the stem are favored systematically. Consequently, if direction-specific climate-growth relationships exist, conventional sampling protocols seeking to avoid reaction wood may unintentionally produce biased chronologies. Therefore, potentially all dendro-ecological and dendro-climatological data sets that were obtained following such standard sampling protocols might be affected.

Increment cores taken from historical and archeological contexts may be particularly sensitive to potential direction-specific bias. This is because, for historical and archaeological wood, the original orientation of the corresponding tree can generally not be determined. Moreover, multiple cores from different – preferably orthogonal – directions are rarely extractable due to the limited accessibility of construction timber in buildings and the artefact-status of wooden archeological objects. Consequently, if direction-specific effects on growth variability and climate-growth relationships exist,

biased chronologies could result. Hence, investigations of direction-specific effects are needed to quantify the bias possibly affecting historic and archaeological data sets that form the backbone of millennia-long chronologies used for climate reconstructions and dendro-provenancing (Bridge, 2012; PAGES 2k Consortium, 2013).

The within- and between-tree sources of noise have been studied from the onset of dendrochronological research (Fritts, 1976). However, systematic investigations of intra-individual growth variability in trees are rare, partly because of the considerable effort needed for collecting sufficient samples to assess tree-growth along the whole stem (Babst et al., 2018; Duncker and Spiecker, 2008). In contrast, growing evidence of direction-specific radial growth was recently documented for several shrub species (Buras and Wilmking, 2014; Shetti et al., 2018; Yang et al., 2018). Moreover, Gričar et al. (2006) showed that heating and cooling of stem sections can affect cambial activity and cell differentiation in *Picea abies* (L.) H. Karst, which may result in direction-specific growth variability if temperature differences between different stem-parts would prevail over several years (but see Buras and Wilmking, 2014 for an elaborated discussion). Changing climatic responses have been documented in stem disk mean chronologies taken at different heights (Chhin et al., 2010). Besides the investigation of Fang et al. (2015), to our knowledge, there exists no other study that reported direction-specific climate-growth relationships in trees among samples taken at the commonly-sampled height of 1.3 m (diameter at breast height).

Potential direction-specific climate-growth relationships could prove problematic, especially if the year-to-year variability was affected. In addition to being the focus of climatological research, high-frequency growth signals – representing the year-to-year

variability – are critical for dendro-provenancing analyses (Gut, 2018). Diverging direction-specific climate-growth relationships, as observed by Fang et al. (2015), thus may result in direction-specific biases that could affect I) the chronologies used for millennia-long climatic reconstructions (PAGES 2k Consortium, 2013), II) the local reference chronologies used for dendro-provenancing and III) the site chronologies established for dendro-ecological studies.

Given the possibly wide-ranging impact on tree-ring research, we here examine the potential for differences in growth variability and climate signals due to the azimuth orientation of tree increment coring. We use tree increment cores from an international tree-ring network that was designed to answer the following research questions:

1. Is there evidence for direction-specific high-frequency growth variability in our data set?

2. Are systematic direction-specific differences in climate-growth relationships present in our data set?

2 Material and methods

2.1 Tree-ring and climate data

To assess possible direction-specific climate signals across different sites and species, the last author of this study (A. Buras) released an international call for contributing tree-ring data in autumn 2017 via the Association of Tree-Ring research (ATR). The sampling followed a uniform design to reduce investigator bias and ensure that cores were

sampled systematically regarding the cardinal direction of the stem. The specifications of the sampling design were: i) 15 trees per site, ii) sampled for two cores from the southern and eastern direction of the stem, iii) collected within a forest, not closer than 100 m to the nearest forest edge of iv) homogeneous, ideally mono-specific forests on v) preferably flat terrain to avoid any potential confounding effects from reaction wood in trees growing on slopes. In addition, for each sampled tree, tree height and diameter at breast height (DBH) were recorded.

All sites met the criteria ii, iii, and v, but at seven sites (THPA, GBPS, REPS, RAPS, AVPN, DPPS, UKPA) less than 15 (minimum twelve) trees were sampled for east- and south-facing increment cores due to the occurrence of wounds or other irregularities and at five sites (OMPS, GBPS, NIPS, CRPG, TLPM) few individuals (in total less than 10% of standing trees) of other tree species were observed. However, since these sites did not reveal differing results in our analyses, we assume possible associated effects to be negligible. All European sites represent managed forests, but the two sites from Canada were located in naturally-grown forests. No data on tree height exists for the sites HCQC and HEQP. For RAPS, DBH was not measured.

Sample preparation, cross-dating and measurement of total ring-widths, as well as quality control of ring-width chronologies, were done following standard dendrochronological procedures (Cook and Kairiukstis, 1990; Grissino-Mayer, 2001; Speer, 2010). Following this protocol, the final data set encompassed 22 sites covering 8 tree species (Table 1, Fig. 1, Fig. 2).

For the series of monthly temperature averages, the 0.5º-gridded CRU TS3.10 data set was used (Harris et al., 2014). For monthly precipitation sums, the 0.5°-gridded GPCC data set was used (Schneider et al., 2016). Tree-ring, climate and tree meta data were analyzed with the statistical software R version 3.5.1 (R Core Team, 2018).

2.2 Preprocessing and signal strength statistics

Given our research question, high-frequency growth variability was the focus of this study. Hence, autoregressive models were fit to the individual ring-width series as derived from the increment cores. The optimal model was chosen as the model that minimized Akaike's Information Criterion (i.e. the default settings of the autoregressive detrending method implemented in the 'dplR' package, Bunn et al., 2018; Bunn, 2008). The resulting series of autoregressive residuals were divided by the mean of the residuals to obtain white noise residual ring-width indices (RWI) with a mean of 1. As a measure of direction-specific signal strength, we computed the mean inter-series Gleichläufigkeit ($\overline{glk}$, Buras and Wilmking, 2015; Eckstein and Bauch, 1969) as well as the mean inter-series correlation ($\bar{r}$, Wigley et al., 1984) pooled by southern and eastern cores. To avoid possible series-length effects, all computations were conducted over the common overlap period of the respective site chronologies. Both statistics were calculated over all possible pairwise comparisons of a respective cardinal direction subset. To bolster robustness, the Spearman's rank sum correlation coefficient was used for all correlation analyses in this study (Best and Roberts, 1975; Hollander et al., 2015).

Besides direction-specific between-series synchronicity, we considered two additional methodological approaches to assess possible direction-specific growth signals: i) direction-specific aggregation of growth signals, and ii) direction-specific climate-growth relationships, which are described in sections 2.3 and 2.4, respectively.

2.3 Principal Component Gradient Analysis

The *Principal Component Gradient Analysis* (PCGA) was proposed by Buras et al. (2016) as a means of detecting subpopulation growth-signals in tree-ring time-series populations. The method is based on the *Principal Component Analysis* (PCA, Mardia et al., 1979; Venables and Ripley, 2002) but focuses on interpreting the polar-transformation of the loadings of the first two principal components (PC1 and PC2) to identify subpopulations of time-series on respective PCGA-plots (Buras et al., 2016).

A PCGA-plot relies on the loadings (arrows) of the typical PCA biplot (e.g. Gower and Hand, 1996). Each of these arrows is representable by the polar transformation (i.e. angle and distance to the origin) of the PC1 and PC2 loadings calculated for the respective time-series (Buras et al., 2016). Based on the polar angles, the underlying time-series are ranked, i.e. sorted with respect to one of the two marginal arrows (Buras et al., 2016). Consequently, one of the two extreme arrows is assigned the rank one, whereas the other is ranked last. The remaining time-series are distributed in between in dependence of their differences in polar angles to the series with the rank one. Distinct, visual groupings of vectors indicate subpopulation signals, provided that PC1 and PC2 explain a reasonable ratio of the variance of the total time-series population.

In the context of this study, PCGA was used to assess the possible occurrence of two direction-specific subpopulations of RWI series (i.e., eastern and southern cores) at each site. To quantitatively identify significant direction-specific growth differences, the angles of the polar coordinates were tested at each site for significant location shifts (from the non-parametric mean rank) via a Wilcoxon Signed-Rank test (Bauer, 1972; Hollander et al., 2015). A paired test was feasible, because for each individual tree, an eastern and southern core were sampled, i.e. the observations were paired. To account for the multiplicity of tests, the p-values were adjusted by controlling the false discovery rate (Benjamini and Hochberg, 1995).

2.4 Climate correlation analysis

Diverging direction-specific climate-growth relationships were studied based on a correlation analysis. This analysis comprised three steps: Firstly, mean site chronologies were computed from the individual, autoregressive residual series to obtain one master chronology per site representative of the corresponding annual average RWI value. Based on these master chronologies, monthly climate correlations (Spearman, see above) were evaluated over a period comprising previous year April to current year October. By investigating climate-correlations to the master chronologies, we ensured that our data set comprised chronologies that are sensitive to climate. If in this step only insignificant climate-correlations were detected, the investigation of direction-specific effects would be rendered obsolete. We considered mean monthly temperature (temp), monthly precipitation sum (prec), and the Standardized Precipitation Evapotranspiration Index (SPEI, Vicente-Serrano et al., 2010) as meaningful climate parameters. The SPEI was integrated over three different time-windows: 1, 3 and 6 months (SPEI1, SPE3,

SPEI6). This accounts for short- and long-term effects of water availability on tree-growth (Vicente-Serrano et al., 2012). For each site, we identified the climate variable(s) with significant correlations to the site chronologies.

Secondly, individual RWI of tree-cores were correlated to the climate variables. The resulting correlation coefficients for respective eastern and southern cores were squared (r^2). The r^2 of a univariate linear regression specifies the variance explained by the regressor (Stock and Watson, 2011). Thus, in our context, r^2 allows for roughly estimating the effect of a given RWI series on a potential reconstruction of the respective climate variable. Hereon, the direction-specific differences in r^2 were investigated via a Wilcoxon Signed-Rank test, which tested the pooled individual differences for eastern and southern cores. Consequently, the test allowed for identifying significant mean differences between eastern and southern cores' r^2 ($\Delta r^2 = r^2_{East} - r^2_{South}$).

Thirdly, the Δr^2 was calculated for each site and visualized with a heatmap. That is, a positive Δr^2 indicates a higher explained variance of eastern cores, whereas a negative Δr^2 indicates a higher explained variance of southern cores. This difference in Δr^2 allows for roughly estimating the effect of the potential direction-specific bias introduced in a potential climate reconstruction. There was a total of 2090 Wilcoxon Signed-Rank tests on Δr^2. Hence, the p-values were adjusted by controlling the false discovery rate (Benjamini and Hochberg, 1995).

3 Results

3.1 Differences in signal strength

Generally, direction-specific differences in signal strength were very small and distributed unsystematically (Fig. 3). The mean difference in $\bar{r}$ between eastern and southern core chronologies (eastern minus southern) was 0.01 (range -0.07 to 0.13). The number of sites that exhibited a lower $\bar{r}$ for eastern cores was equal to the number of sites with a lower $\bar{r}$ for southern cores (ratio 0.5). For $\overline{glk}$, the mean difference was 0.004 (range -0.03 to 0.06). In addition, the number of sites that showed a lower $\overline{glk}$ for eastern cores than for southern cores almost equaled the number of sites, which showed the opposite (ratio 0.45).

3.2 Direction-specific differences according to PCGA

The ratio of variance explained by PC1 and PC2 was on average 0.56 (range 0.35 to 0.77). The ratio was $\leq$ 0.5 for only 6 sites (i.e., ABPA, DPPS, GAPA, JAPS, REPS and ROQR), with only one site (DPPS) below 0.4 (Fig. 4).

The Wilcoxon Signed-Rank tests detected no significant ($p \leq 0.05$) shifts in the polar angles of the PCGA ranks. Moreover, the PCGA-plots showed no distinct visual groupings of the PCGA ranks (Fig. 4).

3.3 Direction-specific differences in climate-growth correlations

At least one climate variable with a significant ($p \leq 0.05$) correlation to the master chronology was detected per site (Fig. A1). Generally, chronologies were positively

299 correlated with current summer precipitation and current summer SPEI1 to SPEI6, and
300 negatively with summer temperature (Fig. A1).

301 Direction-specific differences (Δr^2) in climate-growth relationships were insignificant
302 according to the Wilcoxon Signed-Rank tests (Fig. 5). The mean Δr^2 per site were rather
303 small (25% quantile: -0.01; 75% quantile: 0.01; range: -0.06 to 0.09) and showed no
304 systematic distribution (Fig. 5).

305 4 Discussion

306 4.1 Multi-national data set shows no evidence of direction-specific
307 tree-ring bias

308 Using a large, multi-species data set with samples derived from sites predominantly
309 representing Europe, we found no evidence for bias due to the cardinal direction of
310 coring. We found virtually no differences between the signal strength statistics for
311 eastern and southern core-chronologies, respectively. Furthermore, the PCGA provided
312 no evidence for direction-specific growth variability. None of the Wilcoxon Signed-Rank
313 tests detected any significant shifts in the polar coordinates. Moreover, the PCGA plots
314 showed no clear visual separation, compared to plots in Buras et al. (2018); Rehschuh
315 et al. (2017). Finally, the absolute differences in climate correlations were marginal
316 (cf. Results), and the Wilcoxon Signed-Rank tests detected no significant, direction-
317 specific differences in Δr^2. These results corroborate the reliability of many existing tree-
318 ring data sets used in several important fields of research. These results further indicate
319 that conventional sampling protocols (two cores at diameter at breast height) do not

introduce any notable direction specific bias in ring-width chronologies. Although many of our sites were mesic and on flat terrain by design (to reduce confounding factors), the large number of sites (22) tested across many countries likely captured a relatively wide range of conditions. Nevertheless, sampling in more extreme environments may show different results.

4.2 Direction-specific growth in previous research

The sites studied by Fang et al. (2015) were dominated by *Pinus tabuliformis* and *Picea purpurea* and mostly located on summits and near cliffs within the semi-arid Chinese Loess Plateau. At such sites, trees are presumably more exposed to environmental factors (e.g. drought stress) than trees at the forest interior (Fritts, 1976; Schweingruber, 1996). Thus, trees might have been more affected by unequal direction-specific exposure to wind and solar radiation than the forest-interior trees studied here. Moreover, if the lack of shade from neighboring trees and the prevailing wind direction are reasonably stable in time, they should result in diverging medium- (3-10 years) to low-frequency (>10 years) growth signals (Cook and Kairiukstis, 1990). However, these medium- to low-frequency signals are removed by high-pass filtering as used in our study. The high-frequency growth signal is linked to yearly weather conditions (Cook and Kairiukstis, 1990; Fritts, 1976). For direction-specific year-to-year growth variability to consistently occur, climatic factors would need to divergently drive yearly radial tree-growth depending on the cardinal direction over the course of several decades. Thus, while factors like different shading and wind exposition possibly cause direction-specific growth to occur in the mid- to low-frequency, the high-frequency signal seems to be largely unaffected by direction-specific growth variability. Still, in extreme environments,

direction-specific effects on the high-frequency growth signal are possible (Buras and Wilmking, 2014; Fang et al., 2015).

For certain shrub species growing in cold tundra ecosystems or forming alpine tree lines, direction-specific growth signals have been reported (Buras and Wilmking, 2014; Shetti et al., 2018; Yang et al., 2018). However, the latter signals were not related to cardinal directions (i.e. geographic exposition). These deviating signals were most likely caused by micro-environmental conditions (Buras and Wilmking, 2014), which may also have been a cause for direction-specific growth in the summit and near-cliff stands studied by Fang et al. (2015).

Consequently, direction-specific growth could occur in extreme environments. Previous studies often focused on diverging growth along the stem rather than on direction-specific growth. For example, Chhin et al. (2010) found changing climatic responses in stem disk mean chronologies taken at different heights and Gričar et al. (2006) showed that heating and cooling of stem sections can affect cambial activity and cell differentiation in *Picea abies*. Thus, research focusing on extremely dry or cold environments could contribute to a more complete assessment of direction-specific growth. In addition, direction-specific climate signals may be investigated in frequencies other than the high-frequency time domain.

4.3 Constraints and limitations of our study

The objective of our study was to evaluate the size of direction-specific climate signals in high-pass filtered RWI series. Instead of stacking several statistical methods, we chose an approach that focuses on the direct assessment of differences in climate correlations

and signal strength. We argue that these differences suffice for estimating the relevance of potential direction-specific growth for climate reconstructions. Moreover, this approach is less prone to the problem of interpreting data derivates that result when chaining several multivariate analyses in a sequence, i.e. using the output of an analysis as direct input to the next analysis. Such chaining risks a stepwise disconnection from the original signal differences present in the raw or detrended data, which in turn can lead to a loss of interpretability of the results. Nonetheless, there are several limitations to our study.

4.3.1 Analysis related limitations

For certain sites (i.e., ABPA, DPPS, GAPA, JAPS, REPS and ROQR) the PC1 and PC2 explained less than 50% of the variance. Therefore, additional PCs may have also held meaningful information. However, each of these additional PCs explained an even lower percentage of variance. Moreover, the implementation of polar coordinates in three dimensions is not easily solved. Thus, we restricted our analyses to PC1 and PC2, which explained a relatively high portion of variance for most of the sites.

The PCGA plots showed no clear visual separation. The two-colored PCGA plot is suboptimal for visualizing the Wilcoxon Signed-Rank test, which tests for significant shifts in angles between the pairs of PCGA vectors from the same tree. If the vector pairs have a systematic order, i.e. the eastern is always above or below the southern in the fan of vectors, respectively, the paired test detects significant shifts. It is impossible to visualize these shifts with only two colors, one for each group of eastern and southern cores. Plots with colored vectors specific to the individual tree would overcome this limitation. In addition, a specific line type could be used to indicate if a vector represents

387 a southern or eastern core. However, such plots quickly become fairly complex and may
388 confuse observers (Fig. A4). Thus, and because no significant shifts in polar coordinates
389 were detected, such plots are not shown here.

390 We used gridded climate data (0.5°) as data from nearby meteorological stations was
391 available just for a minority of sites. The gridded data sets only approximately represent
392 the actual climatic conditions at the sites. Thus, the respective climate-growth
393 relationships could have been underestimated for sites that lie in areas with high micro-
394 climatic variability.

395 **4.3.2 Material/sampling related limitations**

396 While there was not always equal representation of species across sites, there is
397 evidence that this does not bias our results. Some species were represented by several
398 sites with differing ecological conditions (e.g. *Pinus sylvestris* L.), whereas for other
399 species we have studied only one site (e.g. *Pseudotsuga menziesii* (Mirb.) Franco). Yet,
400 the well-represented species (e.g. *Pinus sylvestris* L.) showed no clear evidence for
401 systematic direction-specific growth variability. In addition, the geographic and ecological
402 gradients covered by our study were vast, albeit biased towards Europe. Bearing the two
403 Canadian sites in mind, we speculate that a wider spatial coverage (i.e., the sampling of
404 more sites) across the Northern Hemisphere would probably not reveal any direction-
405 specific biases for relatively mesic sites within flat terrain forests.

406 We only investigated two cores per tree. Nevertheless, the two major factors that
407 potentially drive direction-specific climate signals in our study area, i.e. solar radiation

from the south and wind from the west (for European sites in flat terrain mainly), should have been detectable by coring the southern and eastern sides of the stem only.

As stated above, we acknowledge that direction-specific growth variability and climate signals might occur in extreme environments. Here, we concentrated on flat terrain forest sites. On slopes, direction-specific growth is influenced by reaction wood, which is a factor that is potentially difficult to quantify. The formation of reaction wood is thought to primarily influence the mid- to low-frequency growth signal (Duncker and Spiecker, 2008). Still, the high-frequency might be affected by reaction wood formation, especially if the physical strain on a stem changes abruptly. In such cases, the climatic effects and the effects related to reaction wood formation are difficult to distinguish and quantify separately (Speer, 2010). Thus, we focused on sites in flat terrain to test the hypothesis of direction-specific climate signals in the high-frequency growth signal of ring-width series.

Finally, the majority of sites represent managed, largely mono-specific forests. It remains to be tested using other data sets, whether our findings are representative for naturally-grown, multi-species forests. However, the two naturally-grown sites in Canada with few individuals of co-dominant tree species revealed similar results as managed European forests. Thus, these results suggest that direction-specific climate signals probably are also negligible for naturally-grown sites similar to the two Canadian sites.

5 Conclusions

This study found no evidence for systematic direction-specific radial growth in high-pass filtered ring-width series. The climate correlations investigated were largely unaffected by direction-specific effects. Hence, the potential for direction-specific bias in ring-width data sets used by the diverse fields of tree-ring research (e.g. the establishment of reference chronologies for dendro-provenancing and millennia-long chronologies for climate reconstructions) seems negligible. At least this appears to be the case for sites that feature similar site conditions to those studied here, i.e. that lie at the forest interior on comparably moderate sites under relatively mesic conditions. Nevertheless, the cardinal direction of core extraction should be documented to control for micro-environmental factors such as the formation of reaction wood due to exposure to a prevailing wind-direction and/or slope inclination.

Direction-specific growth could prove to be more pronounced at extreme (cold or dry) sites, where trees and shrubs are more exposed to severe weather conditions. Thus, the possible consequences of direction-specific growth on dendrochronological studies in extreme environments would make an excellent avenue for future research to evaluate methodologies and data sets at species margins.

Data availability

The tree-ring and meta data sets are available upon request.

Author contribution statement

The scientific concept and research question of this study was developed in collaboration by A. Buras and U. Gut. The latter also conducted the bulk of the analyses presented here. A. Buras initiated the tree-ring data network. Both together have worked on the submitted manuscript. All other members of the network are listed alphabetically as co-authors, with the exception of Ute Sass-Klaassen, who hosted the first network workshop at Wageningen University and Research. These co-authors contributed to the article by providing tree-ring data sets and valuable feedback at various stages of data analyses as well as commenting on the final manuscript version before submission. We are very grateful for the financial support provided by the Association of Tree-ring Research (ATR), which allowed the implementation of a network-internal statistical workshop.

Acknowledgements

U. Gut thanks N. Bleicher for comments and discussions. U. Gut was financially supported by the Swiss National Science Foundation, grant no. P0ZHP1_162299. A. Buras received funding from the German Academic Exchange Service (DAAD). J. J. Camarero acknowledges the support of the CGL2015-69186-C2-1-R project (Spanish Ministry of Economy). R. Cruz-García was supported by a DAAD-Conacyt scholarship. A. Hevia was supported by OLDPINE (AGL2017-83828-C2-2R) project (Spanish Ministry of Economy, Industry and Competitiveness, MINECO). M. Isaac-Renton and D. Montwé thank Anne-Marie Marchi, Todd Golumbia and CRD Regional parks for sampling permission. T. Kolář and M. Rybníček were supported by the Ministry of

Education, Youth, and Sports of CR within the National Sustainability Program I (NPUI), grant number LO1415, the Czech Science Foundation (18-17295S). A.M. Petritan was supported by the Ministry of Research and Innovation, CNCS – UEFISCDI, project number PN-III-P1-1.1-TE-2016-1508, within PNCDI III (BIOCARB). R. Sánchez-Salguero was supported by the projects CoMo-ReAdapt (CGL2013-48843-C2-1-R, Spanish Ministry of Economy, Industry and Competitiveness, Spain) and LESENS (RTI2018-096884-B-C33, Ministry of Science, Innovation and Universities, Spain).

Figures

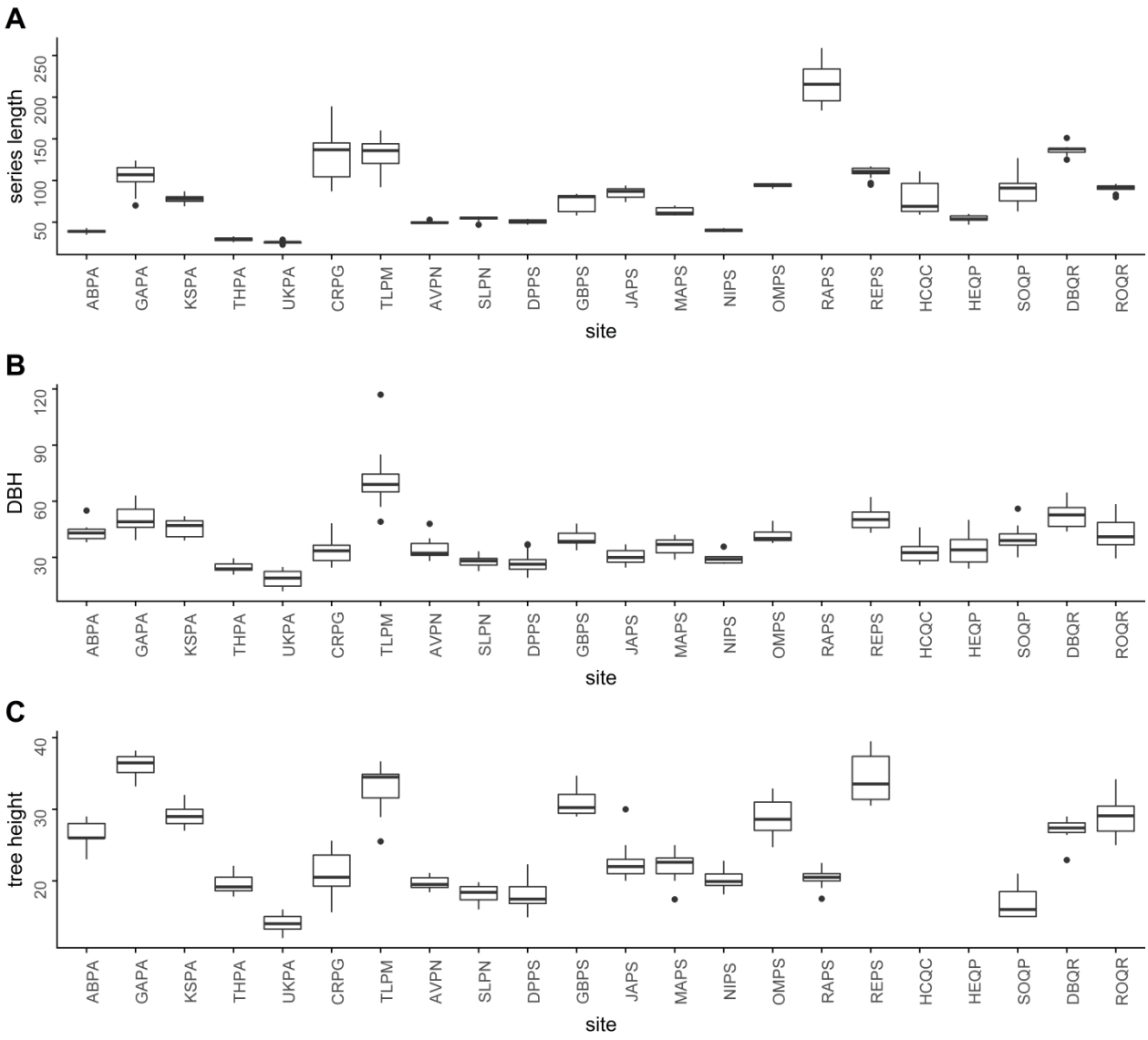

Fig. 1: Descriptive statistics of the studied sites. A: Length of ring-width series in years (per tree only the longer series among the eastern and southern core series was included). B: Diameter at breast height (DBH) in cm. C: Tree height in m. Sites are sorted by species. The last two letters of the site abbreviations provide the species abbreviations (see Table 1).

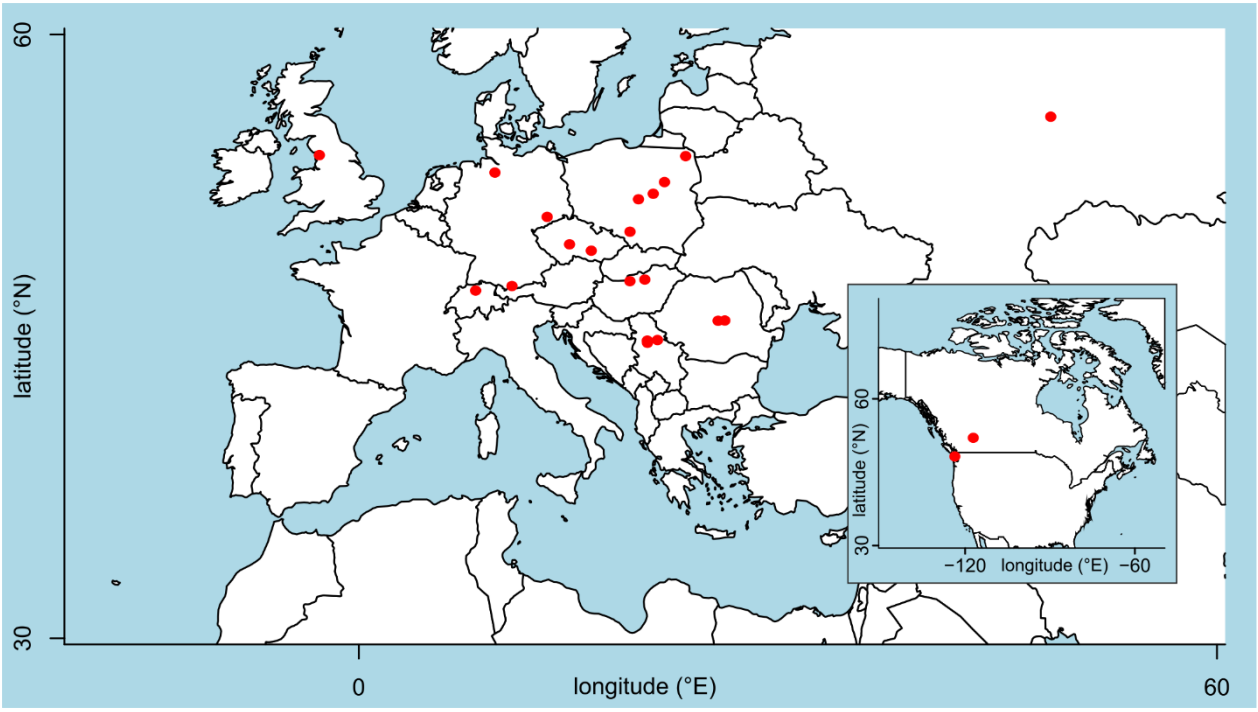

Fig. 2: Geographical location of the study sites (red points) in Europe. Moreover, the study includes two sites located in Canada (inset map). For more meta data see Table 1.

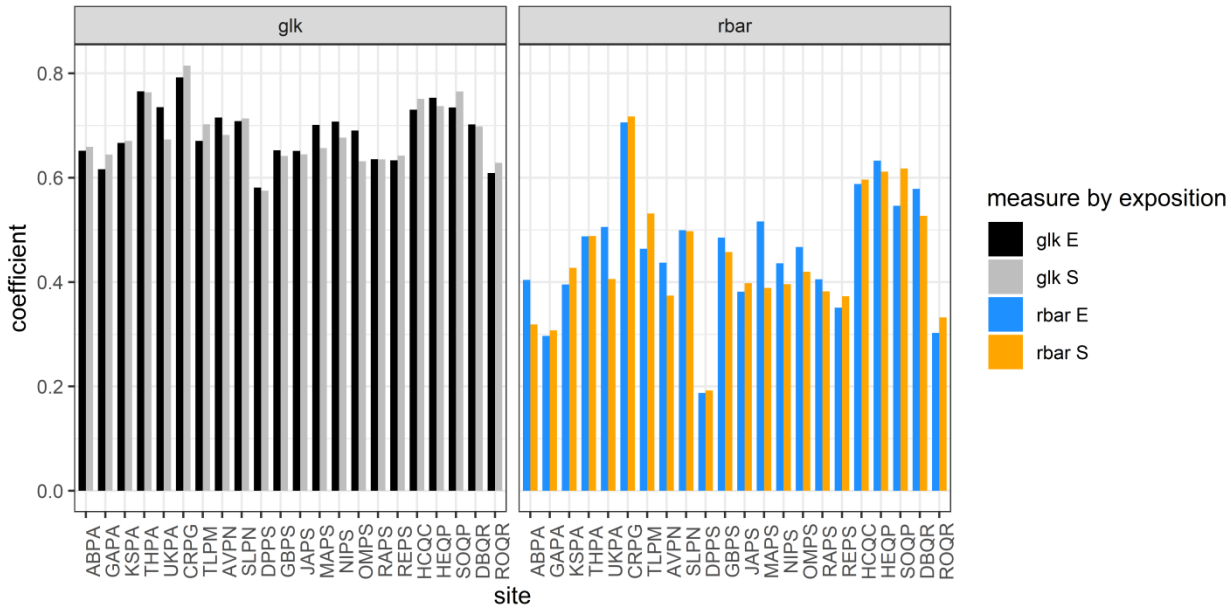

Fig. 3: Direction-specific differences in signal strength between eastern (E) and southern (S) tree cores per site (abbreviations Table 1). Measures are Gleichläufigkeit (glk) and mean inter-series correlation (rbar). Sites are sorted by species.

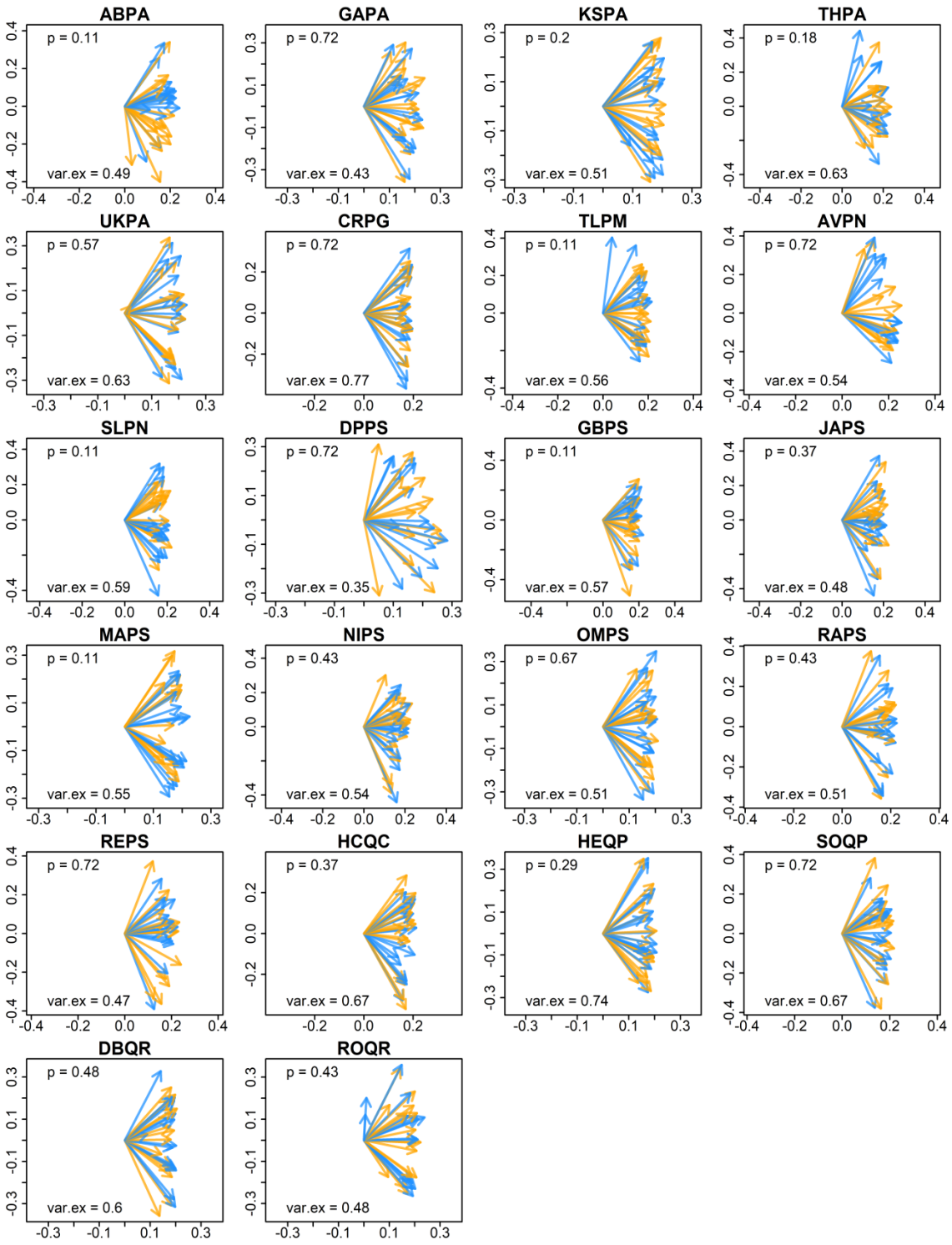

490

491 *Fig. 4: Direction-specific differences in growth variability according to PCGA. P: p-value*
492 *of Wilcoxon Signed-Rank tests. Var.ex: Ratio of variance explained by PC1 and PC2.*
493 *Orange arrows refer to southern, blue arrows to eastern tree cores. Sites are sorted by*
494 *species (abbreviations Table 1).*

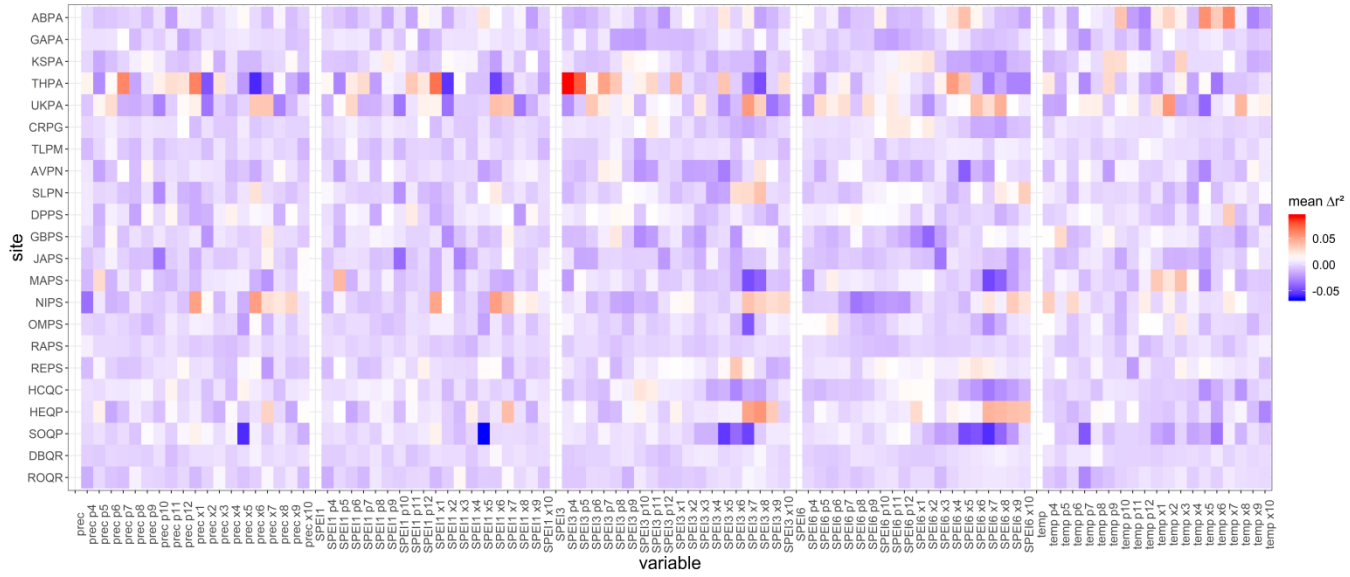

495

496 *Fig. 5: Mean Δr^2 between eastern and southern cores climate-growth correlations per*
497 *site and climate variable. None of the Wilcoxon Signed-Rank tests on Δr^2 was significant*
498 *($p \leq 0.05$) after adjusting for the multiplicity of tests. SPEI is the Standardized*
499 *Precipitation Evapotranspiration Index, temp is mean monthly temperature, prec is total*
500 *monthly precipitation. A 'p' preceding the number of the month (x-axis labels) denotes*
501 *previous year observations of the respective climate variable. An 'x' preceding the*
502 *number of the month denotes current year observations. Sites are sorted by species*
503 *(abbreviations Table 1).*

Tables

Table 1: Meta data summary for all sites and species included in the study. Sites are sorted by country. Latitude and longitude in decimal degrees. N: Number of trees for which an eastern and a southern core was sampled; 1st yr, Last yr: First and last year of the common overlap period shared by all ring-width series of a site; M.s.length: Mean series length in years (calculated across eastern and southern cores); M.DBH: Mean diameter at breast height in cm; M.height: Mean tree height in m. Temp: Mean annual temperature in °C; Prec: Mean yearly precipitation sums in mm.

Country	Site	Abbrev.	Species	Latitude	Longitude (-W, +E)	N	1st yr	Last yr	M.s.length	M.DBH	M.height	Temp	Prec
Canada	Cline River	CRPG	*Picea glauca* (Moench) Voss	52.000	-116.507	15	1940	2017	121	34	21	-2.1	664
Canada	Thetis Lake	TLPM	*Pseudotsuga menziesii* (Mirb.) Franco	48.462	-123.465	15	1928	2017	129	72	33	9.3	720
Czech Republic	Košetice	KSPA	*Picea abies* (L.) H.Karst.	49.566	15.091	15	1962	2017	75	45	29	7.8	626
Czech Republic	Soběšice	SOQP	*Quercus petraea* (Matt.) Liebl.	49.250	16.610	15	1984	2014	87	40	17	8.1	569
Germany	Garmisch	GAPA	*Picea abies* (L.) H.Karst.	47.494	11.065	15	1963	2017	97	51	36	3.1	1051
Germany	Niederhaverbek	NIPS	*Pinus sylvestris* L.	53.132	9.875	15	1984	2017	40	29	20	8.7	743
Germany	Tharandt	THPA	*Picea abies* (L.) H.Karst.	50.929	13.526	14	1997	2017	28	25	20	8.0	788
Hungary	Puspokszilagy	HCQC	*Quercus cerris* L.	47.752	19.302	15	1966	2017	77	34	NA	9.2	596
Hungary	Kerecsend	HEQP	*Quercus petraea* (Matt.) Liebl.	47.815	20.354	15	1977	2015	52	35	NA	9.8	583
Poland	Gleboki Brod	GBPS	*Pinus sylvestris* L.	53.950	23.210	14	1966	2017	73	40	31	6.9	564
Poland	Jaworzno	JAPS	*Pinus sylvestris* L.	50.194	19.315	15	1964	2017	82	30	22	8.2	731
Poland	Magdalenka	MAPS	*Pinus sylvestris* L.	52.080	20.941	15	1970	2017	62	36	22	8.2	542
Poland	Ostrow	OMPS	*Pinus sylvestris* L.	52.660	21.730	15	1960	2017	92	42	29	7.8	584
Poland	Rogów	ROQR	*Quercus robur* L.	51.806	19.911	15	1950	2016	86	42	29	8.1	585
Romania	Dumbravita	DBQR	*Quercus robur* L.	45.769	25.478	15	1903	2017	132	52	27	7.6	716
Romania	Reci	REPS	*Pinus sylvestris* L.	45.816	25.943	14	1959	2016	107	50	34	7.8	665
Russia	Raifa	RAPS	*Pinus sylvestris* L.	55.909	48.733	14	1900	1981	202	NA	20	3.9	527
Serbia	Avala	AVPN	*Pinus nigra* J.F.Arnold	44.672	20.541	12	1977	2017	49	34	20	12.0	642
Serbia	Deliblatski Pesak	DPPS	*Pinus sylvestris* L.	44.811	21.239	14	1976	2017	50	27	18	11.7	641
Serbia	Stepin Lug	SLPN	*Pinus nigra* J.F.Arnold	44.748	20.531	15	1976	2017	53	28	18	12.0	642
Switzerland	Albisboden	ABPA	*Picea abies* (L.) H.Karst.	47.269	8.525	15	1990	2017	37	43	27	8.3	1435
United Kingdom	North England	UKPA	*Picea abies* (L.) H.Karst.	54.000	-2.400	14	1998	2017	25	18	14	8.6	1273

References

Amoroso, M.M., Daniels, L.D., Baker, P.J., Camarero, J.J. (Eds.), 2017. Dendroecology: Tree-ring analyses applied to ecological studies. Springer, Cham, 400 pp.

Babst, F., Bodesheim, P., Charney, N., Friend, A.D., Girardin, M.P., Klesse, S., Moore, D.J.P., Seftigen, K., Björklund, J., Bouriaud, O., Dawson, A., DeRose, R.J., Dietze, M.C., Eckes, A.H., Enquist, B., Frank, D.C., Mahecha, M.D., Poulter, B., Record, S., Trouet, V., Turton, R.H., Zhang, Z., Evans, M.E.K., 2018. When tree rings go global: Challenges and opportunities for retro- and prospective insight. Quaternary Science Reviews 197, 1–20. 10.1016/j.quascirev.2018.07.009.

Bauer, D.F., 1972. Constructing Confidence Sets Using Rank Statistics. Journal of the American Statistical Association 67 (339), 687–690. 10.1080/01621459.1972.10481279.

Benjamini, Y., Hochberg, Y., 1995. Controlling the False Discovery Rate: A Practical and Powerful Approach to Multiple Testing. Journal of the Royal Statistical Society 57 (1), 289–300.

Best, D.J., Roberts, D.E., 1975. Algorithm AS 89: The Upper Tail Probabilities of Spearman's Rho. Journal of the Royal Statistical Society 24 (3), 377. 10.2307/2347111.

Bleicher, N., Harb, C. (Eds.), 2015. Zürich-Parkhaus Opéra: Eine neolithische Feuchtbodenfundstelle. FO-Fotorotar, Zürich, Egg, 270 pp.

Bridge, M., 2012. Locating the origins of wood resources: a review of dendroprovenancing. Journal of Archaeological Science 39 (8), 2828–2834. 10.1016/j.jas.2012.04.028.

Bunn, A.G., 2008. A dendrochronology program library in R (dplR). Dendrochronologia 26 (2), 115–124. 10.1016/j.dendro.2008.01.002.

538 Bunn, A., Korpela, M., Biondi, F., Campelo, F., Mérian, P., Qeadan, F., Zang, C., Pucha-
539 Cofrep, D., Wernicke, J., 2018. dplR: Dendrochronology Program Library in R.

540 Buras, A., Schunk, C., Zeiträg, C., Herrmann, C., Kaiser, L., Lemme, H., Straub, C.,
541 Taeger, S., Gößwein, S., Klemmt, H.-J., Menzel, A., 2018. Are Scots pine forest
542 edges particularly prone to drought-induced mortality? Environ. Res. Lett. 13 (2),
543 25001. 10.1088/1748-9326/aaa0b4.

544 Buras, A., van der Maaten-Theunissen, M., van der Maaten, E., Ahlgrimm, S., Hermann,
545 P., Simard, S., Heinrich, I., Helle, G., Unterseher, M., Schnittler, M., Eusemann,
546 P., Wilmking, M., 2016. Tuning the Voices of a Choir: Detecting Ecological
547 Gradients in Time-Series Populations. PloS one 11 (7), e0158346.
548 10.1371/journal.pone.0158346.

549 Buras, A., Wilmking, M., 2014. Straight lines or eccentric eggs? A comparison of radial
550 and spatial ring width measurements and its implications for climate transfer
551 functions. Dendrochronologia 32 (4), 313–326. 10.1016/j.dendro.2014.07.002.

552 Buras, A., Wilmking, M., 2015. Correcting the calculation of Gleichläufigkeit.
553 Dendrochronologia 34, 29–30. 10.1016/j.dendro.2015.03.003.

554 Carrer, M., 2011. Individualistic and time-varying tree-ring growth to climate sensitivity.
555 PloS one 6 (7), e22813. 10.1371/journal.pone.0022813.

556 Chhin, S., Hogg, E.H.T., Lieffers, V.J., Huang, S., 2010. Growth-climate relationships
557 vary with height along the stem in lodgepole pine. Tree physiology 30 (3), 335–
558 345. 10.1093/treephys/tpp120.

559 Cook, E.R., Kairiukstis, L.A., 1990. Methods of Dendrochronology. Springer
560 Netherlands, Dordrecht.

561 Duncker, P., Spiecker, H., 2008. Cross-sectional compression wood distribution and its
562 relation to eccentric radial growth in Picea abies [L.] Karst. Dendrochronologia 26
563 (3), 195–202. 10.1016/j.dendro.2008.06.004.

564 Eckstein, D., Bauch, J., 1969. Beitrag zur Rationalisierung eines dendrochronologischen
565 Verfahrens und zur Analyse seiner Aussagesicherheit. Forstwissenschaftliches
566 Centralblatt 88, 230–250.

567 Eissing, T., Dittmar, C., 2011. Timber transport and dendroprovenancing in Thuringia
568 and Bavaria., in: Treerings, Art and Archaeology, pp. 137–149.

569 Fang, K., Chen, D., Gou, X., D'Arrigo, R., Davi, N., 2015. Influence of non-climatic
570 factors on the relationships between tree growth and climate over the Chinese
571 Loess Plateau. Global and Planetary Change 132, 54–63.
572 10.1016/j.gloplacha.2015.06.008.

573 Fritts, H.C., 1976. Tree Rings and Climate. Elsevier.

574 Galván, J.D., Camarero, J.J., Gutiérrez, E., 2014. Seeing the trees for the forest: drivers
575 of individual growth responses to climate in Pinus uncinata mountain forests. J
576 Ecol 102 (5), 1244–1257. 10.1111/1365-2745.12268.

577 Gower, J.C., Hand, D.J., 1996. Biplots, 1st ed. Chapman & Hall, London, 277 pp.

578 Gričar, J., Zupancic, M., Cufar, K., Koch, G., Schmitt, U., Oven, P., 2006. Effect of local
579 heating and cooling on cambial activity and cell differentiation in the stem of
580 Norway spruce (Picea abies). Annals of botany 97 (6), 943–951.
581 10.1093/aob/mcl050.

582 Grissino-Mayer, H., 2001. Evaluating crossdating accuracy: a manual and tutorial for the
583 computer program COFECHA. Tree-Ring Research 57.

584 Gut, U., 2018. Evaluating the key assumptions underlying dendro-provenancing: How to
585 spruce it up with a scissor plot. Dendrochronologia 52, 131–145.
586 10.1016/j.dendro.2018.09.008.

587 Harris, I., Jones, P.D., Osborn, T.J., Lister, D.H., 2014. Updated high-resolution grids of
588 monthly climatic observations - the CRU TS3.10 Dataset. Int. J. Climatol. 34 (3),
589 623–642. 10.1002/joc.3711.

590 Hollander, M., A. Wolfe, D., Chicken, E., 2015. Nonparametric Statistical Methods. John
591 Wiley & Sons, Inc, Hoboken, NJ, USA.

592 Hughes, M.K., Swetnam, T.W., Diaz, H.F., 2011. Dendroclimatology. Springer
593 Netherlands, Dordrecht.

594 Klesse, S., DeRose, R.J., Guiterman, C.H., Lynch, A.M., O'Connor, C.D., Shaw, J.D.,
595 Evans, M.E.K., 2018. Sampling bias overestimates climate change impacts on
596 forest growth in the southwestern United States. Nature communications 9 (1),
597 5336. 10.1038/s41467-018-07800-y.

598 Mardia, K.V., Kent, J.T., Bibby, J.M., 1979. Multivariate analysis. Acad. Press, London,
599 521 pp.

600 Melvin, T.M., Briffa, K.R., 2008. A “signal-free” approach to dendroclimatic
601 standardisation. Dendrochronologia 26 (2), 71–86.
602 10.1016/j.dendro.2007.12.001.

603 PAGES 2k Consortium, 2013. Continental-scale temperature variability during the past
604 two millennia. Nature Geosci 6 (5), 339–346. 10.1038/ngeo1797.

605 Peters, R.L., Groenendijk, P., Vlam, M., Zuidema, P.A., 2015. Detecting long-term
606 growth trends using tree rings: a critical evaluation of methods. Global change
607 biology 21 (5), 2040–2054. 10.1111/gcb.12826.

608 R Core Team. R: A Language and Environment for Statistical Computing: R Foundation
609 for Statistical Computing, Vienna, Austria.

610 Rehschuh, R., Mette, T., Menzel, A., Buras, A., 2017. Soil properties affect the drought
611 susceptibility of Norway spruce. Dendrochronologia 45, 81–89.
612 10.1016/j.dendro.2017.07.003.

613 Schneider, U., Becker, A., Finger, P., Meyer-Christoffer, A., Rudolf, B., Ziese, M. GPCC
614 Full Data Reanalysis Version 7.0: Monthly Land-Surface Precipitation from Rain
615 Gauges built on GTS based and Historic Data.

616 Schweingruber, F.H., 1996. Tree rings and environment dendroecology. Haupt, Berne,
617 Stuttgart, Vienna, 609 pp.

618 Shetti, R., Buras, A., Smiljanic, M., Wilmking, M., 2018. Climate sensitivity is affected by
619 growth differentiation along the length of Juniperus communis L. shrub stems in
620 the Ural Mountains. Dendrochronologia 49, 29–35.
621 10.1016/j.dendro.2018.02.006.

622 Speer, J.H., 2010. Fundamentals of tree-ring research. Univ. of Arizona Press, Tucson,
623 Ariz., 333 pp.

624 Stock, J.H., Watson, M.W., 2011. Introduction to econometrics, 3rd ed. Pearson/Addison
625 Wesley, Boston, XLII, 785.

626 Sullivan, P.F., Csank, A.Z., 2016. Contrasting sampling designs among archived
627 datasets: implications for synthesis efforts. Tree physiology 36 (9), 1057–1059.
628 10.1093/treephys/tpw067.

629 Venables, W.N., Ripley, B.D., 2002. Modern Applied Statistics with S. Springer, New
630 York, NY, 497 pp.

631 Vicente-Serrano, S.M., Beguería, S., López-Moreno, J.I., 2010. A Multiscalar Drought
632 Index Sensitive to Global Warming: The Standardized Precipitation
633 Evapotranspiration Index. J. Climate 23 (7), 1696–1718.
634 10.1175/2009JCLI2909.1.

635 Vicente-Serrano, S.M., Beguería, S., Lorenzo-Lacruz, J., Camarero, J.J., López-Moreno,
636 J.I., Azorin-Molina, C., Revuelto, J., Morán-Tejeda, E., Sanchez-Lorenzo, A.,
637 2012. Performance of Drought Indices for Ecological, Agricultural, and
638 Hydrological Applications. Earth Interact. 16 (10), 1–27.
639 10.1175/2012EI000434.1.

640 Wigley, T.M.L., Briffa, K.R., Jones, P.D., 1984. On the Average Value of Correlated
641 Time Series, with Applications in Dendroclimatology and Hydrometeorology. J.
642 Climate Appl. Meteor. 23 (2), 201–213. 10.1175/1520-
643 0450(1984)023<0201:OTAVOC>2.0.CO;2.

WMO (1989) Calculation of Monthly and Annual 30-Year Standard Normals, WCDP-No. 10, WMO-TD/No. 341. Geneva: World Meteorological Organization.

Yang, J., Zhao, H., Zhang, Y., Li, Z., Wang, X., 2018. Climate–growth relationship for different directions of Pinus pumila radial growth at the treeline of northern Daxing'an Mountains, China. Trees 32 (1), 311–322. 10.1007/s00468-017-1633-4.

A

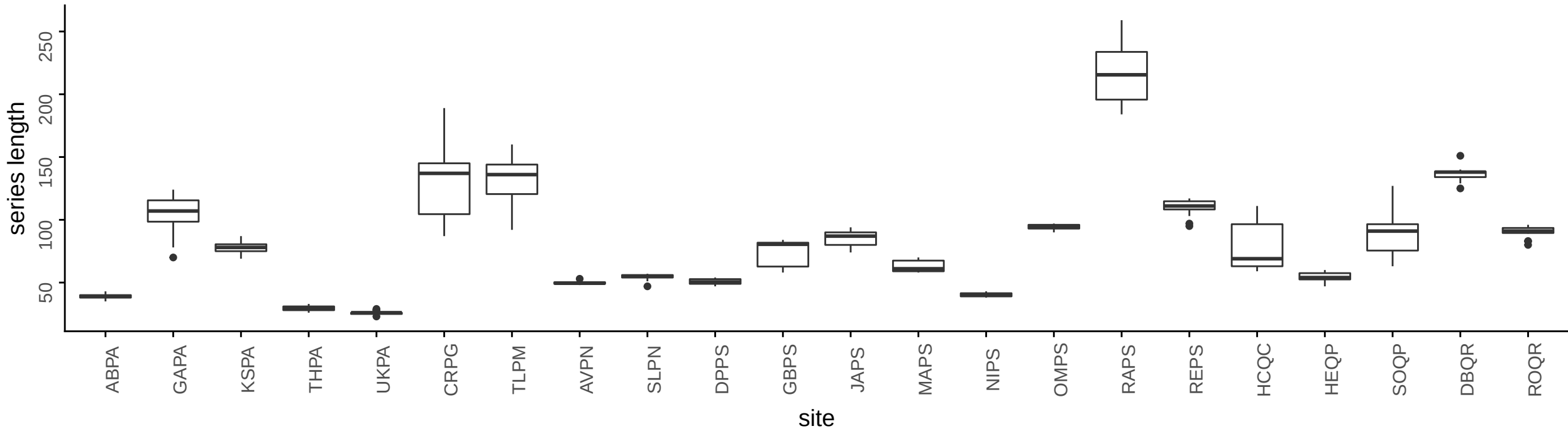
series length
50
100
150
200
250
ABPA
GAPA
KSPA
THPA
UKPA
CRPG
TLPM
AVPN
SLPN
DPPS
GBPS
JAPS
MAPS
NIPS
OMPS
RAPS
REPS
HCQC
HEQP
SOQP
DBQR
ROQR
site

B

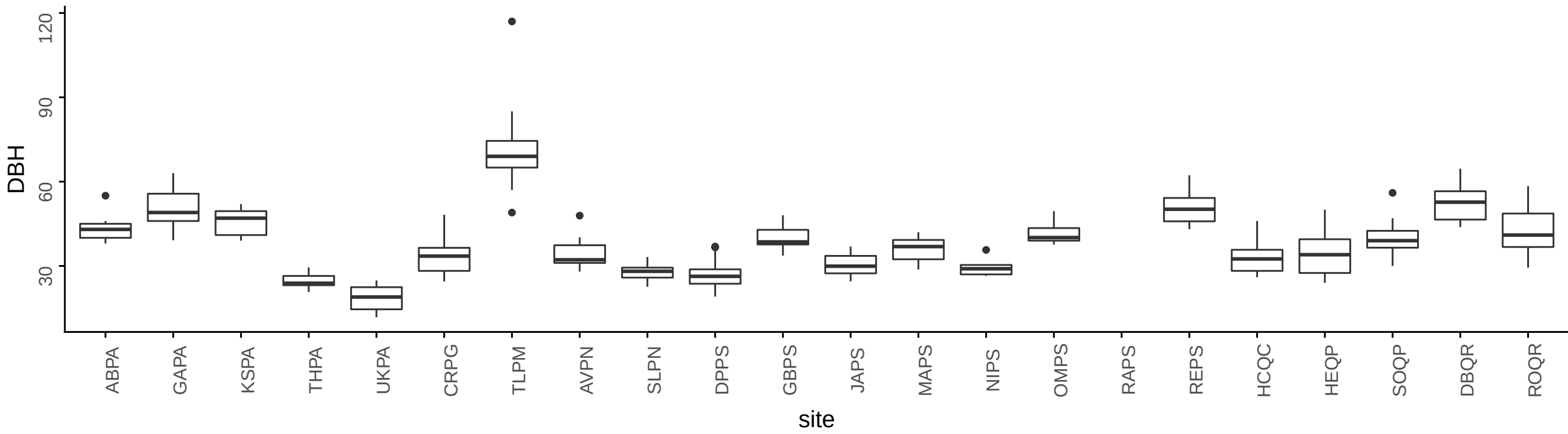
DBH
30
60
90
120
ABPA
GAPA
KSPA
THPA
UKPA
CRPG
TLPM
AVPN
SLPN
DPPS
GBPS
JAPS
MAPS
NIPS
OMPS
RAPS
REPS
HCQC
HEQP
SOQP
DBQR
ROQR
site

C

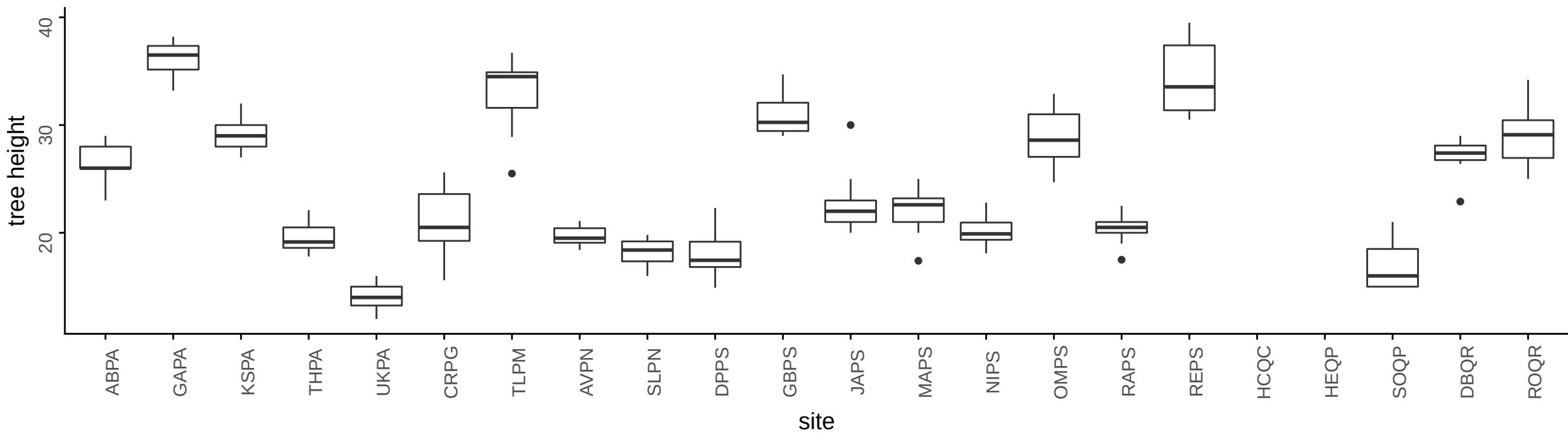
tree height
20
30
40
ABPA
GAPA
KSPA
THPA
UKPA
CRPG
TLPM
AVPN
SLPN
DPPS
GBPS
JAPS
MAPS
NIPS
OMPS
RAPS
REPS
HCQC
HEQP
SOQP
DBQR
ROQR
site

Fig. 1: Descriptive statistics of the studied sites. A: Length of ring-width series in years (per tree only the longer series among the eastern and southern core series was included). B: Diameter at breast height (DBH) in cm. C: Tree height in m. Sites are sorted by species. The last two letters of the site abbreviations provide the species abbreviations (see Table 1).

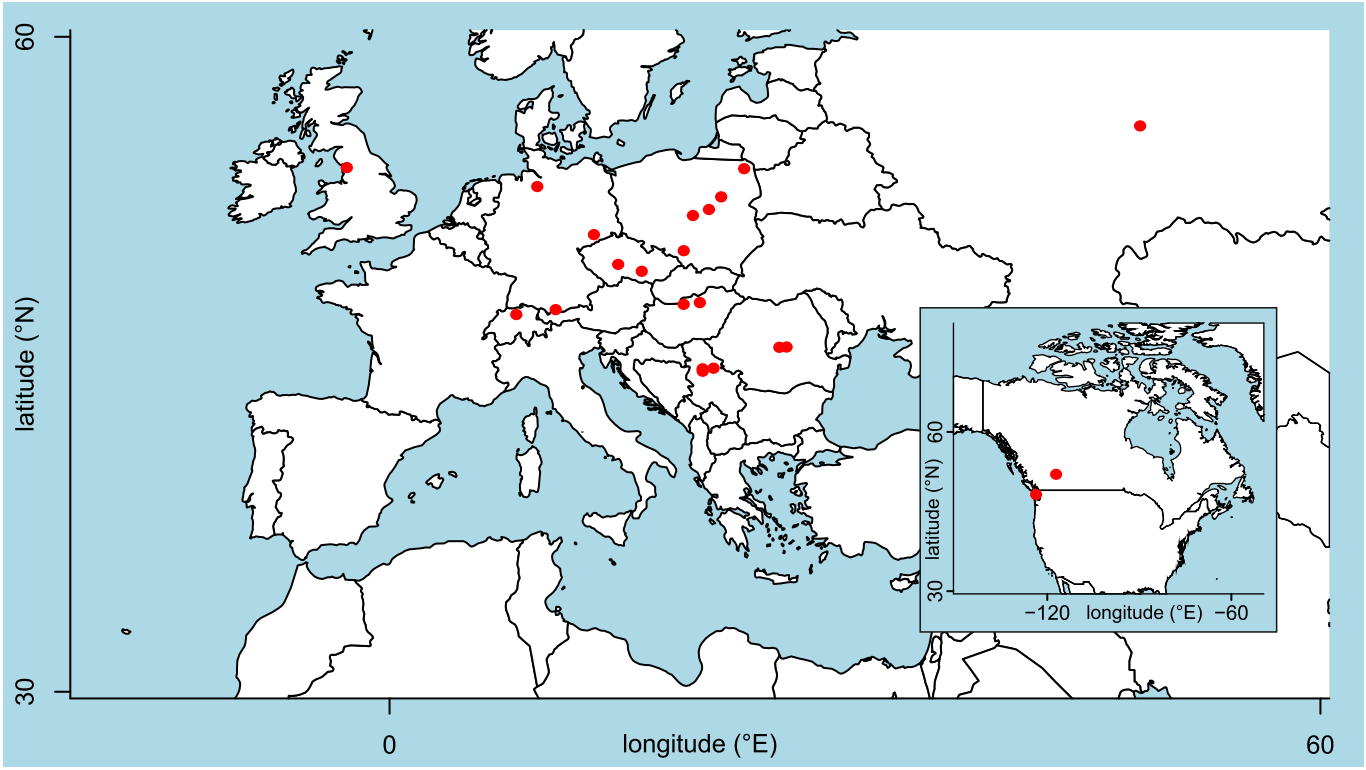
60
latitude (°N)
30
0
longitude (°E)
60
60
latitude (°N)
30
−120
longitude (°E)
−60

Fig. 2: Geographical location of the study sites (red points) in Europe. Moreover, the study includes two sites located in Canada (inset map). For more meta data see Table 1.

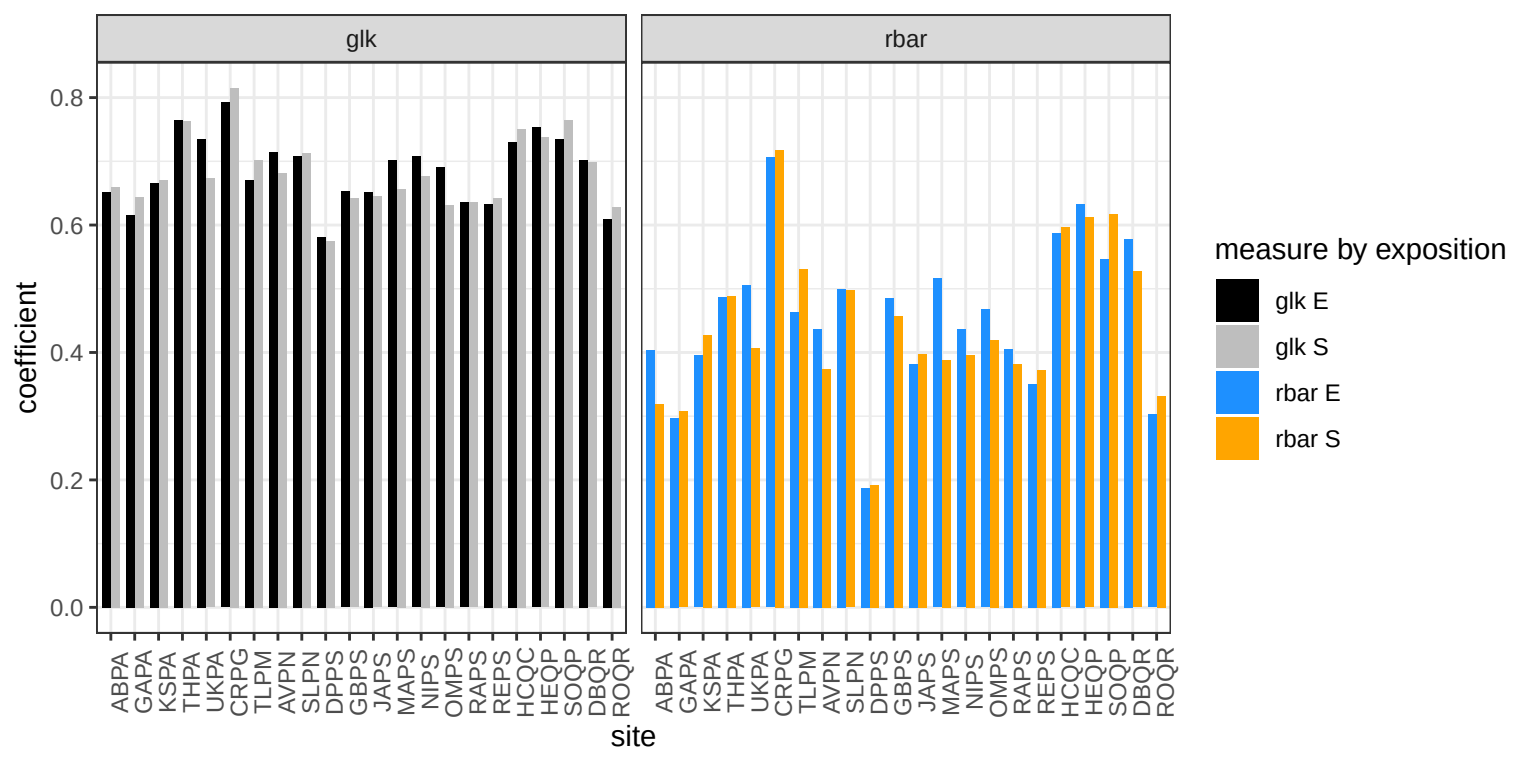
glk
rbar
coefficient
0.0
0.2
0.4
0.6
0.8
ABPA
GAPA
KSPA
THPA
UKPA
CRPG
TLPM
AVPN
SLPN
DPPS
GBPS
JAPS
MAPS
NIPS
OMPS
RAPS
REPS
HCQC
HEQP
SOQP
DBQR
ROQR
site
measure by exposition
glk E
glk S
rbar E
rbar S

Fig. 3: Direction-specific differences in signal strength between eastern (E) and southern (S) tree cores per site (abbreviations Table 1). Measures are Gleichläufigkeit (glk) and mean inter-series correlation (rbar). Sites are sorted by species.

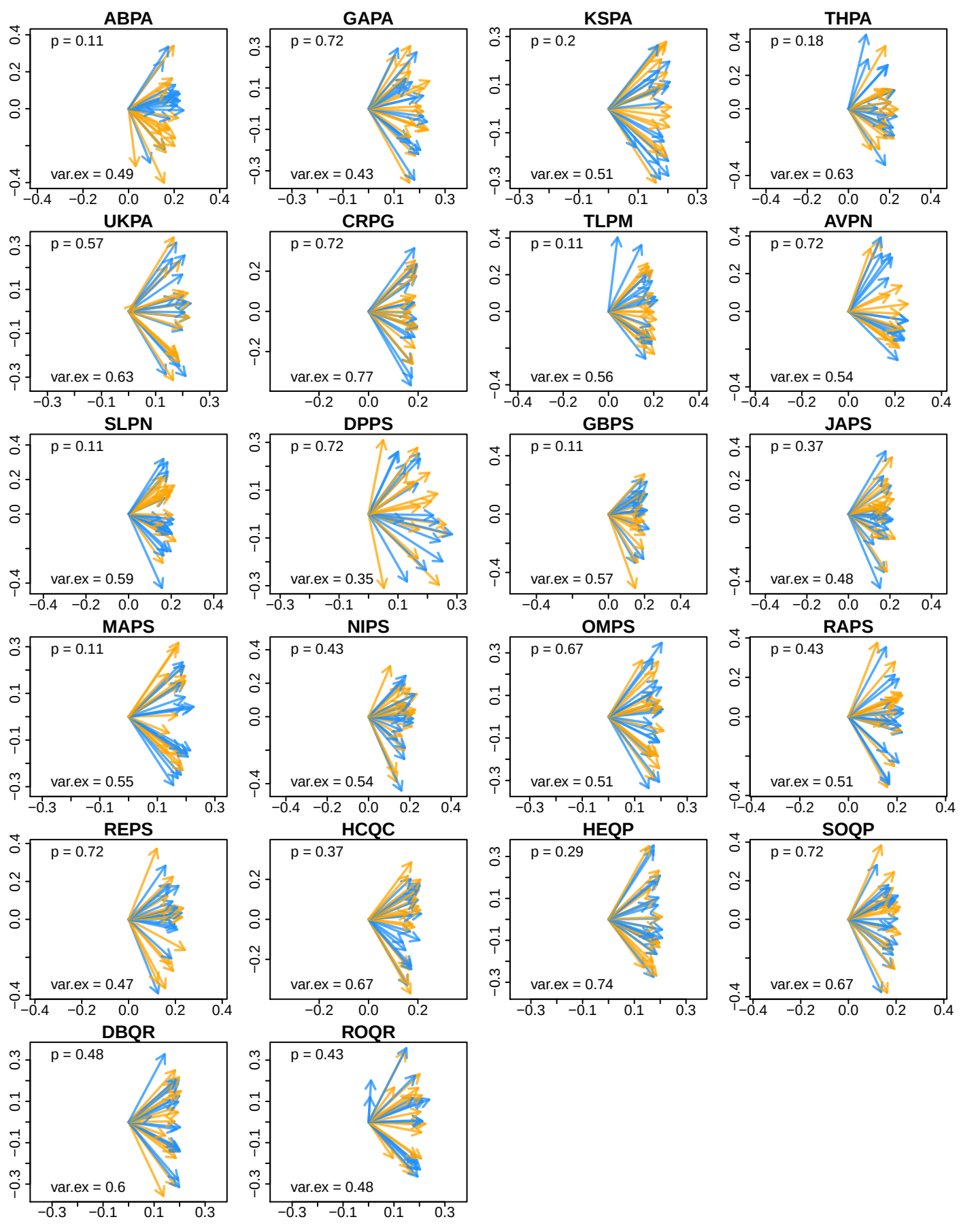
ABPA
p = 0.11
var.ex = 0.49
GAPA
p = 0.72
var.ex = 0.43
KSPA
p = 0.2
var.ex = 0.51
THPA
p = 0.18
var.ex = 0.63
UKPA
p = 0.57
var.ex = 0.63
CRPG
p = 0.72
var.ex = 0.77
TLPM
p = 0.11
var.ex = 0.56
AVPN
p = 0.72
var.ex = 0.54
SLPN
p = 0.11
var.ex = 0.59
DPPS
p = 0.72
var.ex = 0.35
GBPS
p = 0.11
var.ex = 0.57
JAPS
p = 0.37
var.ex = 0.48
MAPS
p = 0.11
var.ex = 0.55
NIPS
p = 0.43
var.ex = 0.54
OMPS
p = 0.67
var.ex = 0.51
RAPS
p = 0.43
var.ex = 0.51
REPS
p = 0.72
var.ex = 0.47
HCQC
p = 0.37
var.ex = 0.67
HEQP
p = 0.29
var.ex = 0.74
SOQP
p = 0.72
var.ex = 0.67
DBQR
p = 0.48
var.ex = 0.6
ROQR
p = 0.43
var.ex = 0.48

Fig. 4: Direction-specific differences in growth variability according to PCGA. P: p-value of Wilcoxon Signed-Rank tests. Var.ex: Ratio of variance explained by PC1 and PC2. Orange arrows refer to southern, blue arrows to eastern tree cores. Sites are sorted by species (abbreviations Table 1).

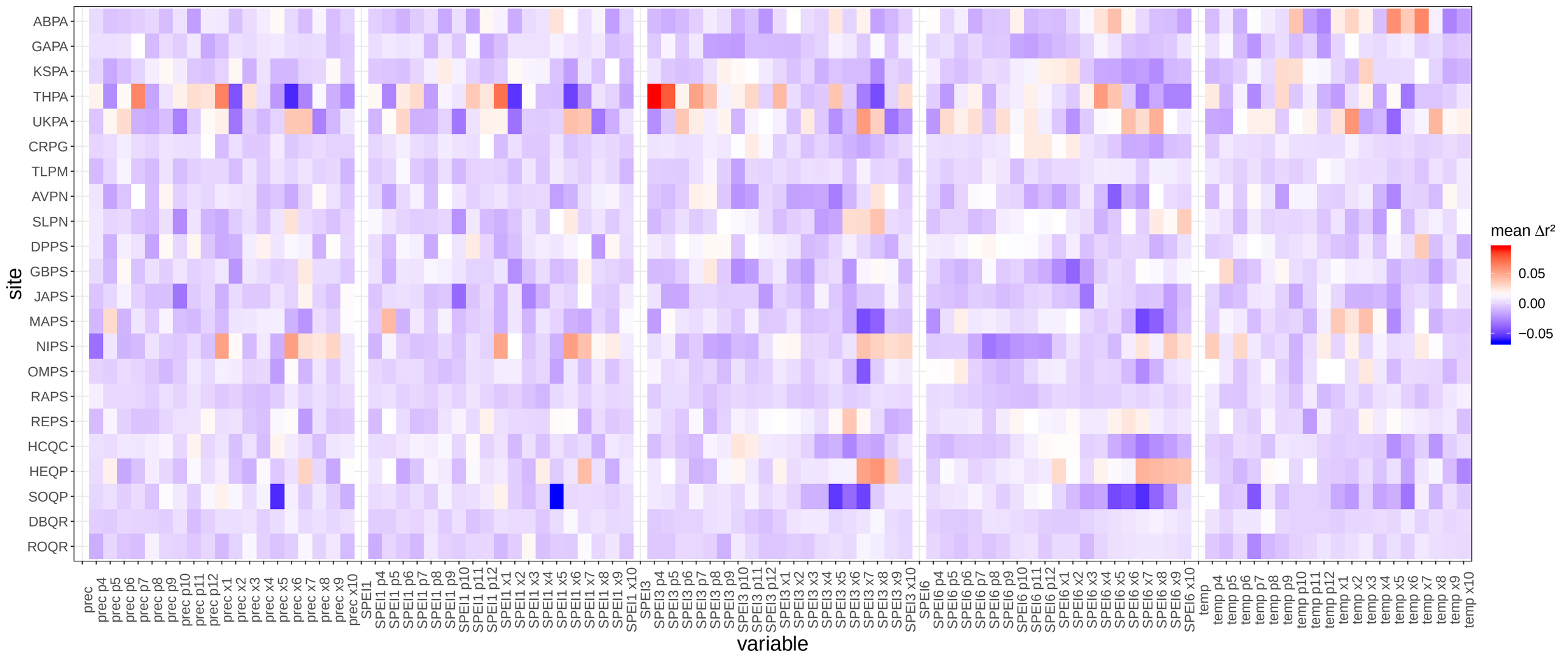
site
ABPA
GAPA
KSPA
THPA
UKPA
CRPG
TLPM
AVPN
SLPN
DPPS
GBPS
JAPS
MAPS
NIPS
OMPS
RAPS
REPS
HCQC
HEQP
SOQP
DBQR
ROQR
variable
prec
prec p4
prec p5
prec p6
prec p7
prec p8
prec p9
prec p10
prec p11
prec p12
prec x1
prec x2
prec x3
prec x4
prec x5
prec x6
prec x7
prec x8
prec x9
prec x10
SPEI1
SPEI1 p4
SPEI1 p5
SPEI1 p6
SPEI1 p7
SPEI1 p8
SPEI1 p9
SPEI1 p10
SPEI1 p11
SPEI1 p12
SPEI1 x1
SPEI1 x2
SPEI1 x3
SPEI1 x4
SPEI1 x5
SPEI1 x6
SPEI1 x7
SPEI1 x8
SPEI1 x9
SPEI1 x10
SPEI3
SPEI3 p4
SPEI3 p5
SPEI3 p6
SPEI3 p7
SPEI3 p8
SPEI3 p9
SPEI3 p10
SPEI3 p11
SPEI3 p12
SPEI3 x1
SPEI3 x2
SPEI3 x3
SPEI3 x4
SPEI3 x5
SPEI3 x6
SPEI3 x7
SPEI3 x8
SPEI3 x9
SPEI3 x10
SPEI6
SPEI6 p4
SPEI6 p5
SPEI6 p6
SPEI6 p7
SPEI6 p8
SPEI6 p9
SPEI6 p10
SPEI6 p11
SPEI6 p12
SPEI6 x1
SPEI6 x2
SPEI6 x3
SPEI6 x4
SPEI6 x5
SPEI6 x6
SPEI6 x7
SPEI6 x8
SPEI6 x9
SPEI6 x10
temp
temp p4
temp p5
temp p6
temp p7
temp p8
temp p9
temp p10
temp p11
temp p12
temp x1
temp x2
temp x3
temp x4
temp x5
temp x6
temp x7
temp x8
temp x9
temp x10
mean Δr²
0.05
0.00
−0.05

Fig. 5: Mean Δr^2 between eastern and southern cores climate-growth correlations per site and climate variable. None of the Wilcoxon Signed-Rank tests on Δr^2 was significant ($p \leq 0.05$) after adjusting for the multiplicity of tests. SPEI is the Standardized Precipitation Evapotranspiration Index, temp is mean monthly temperature, prec is total monthly precipitation. A 'p' preceding the number of the month (x-axis labels) denotes previous year observations of the respective climate variable. An 'x' preceding the number of the month denotes current year observations. Sites are sorted by species (abbreviations Table 1).

Country	Site	Abbrev.	Species	Latitude	Longitude (-W, +E)	N	1st yr	Last yr	M.s.length	M.DBH	M.height	Temp	Prec
Canada	Cline River	CRPG	*Picea glauca* (Moench) Voss	52.000	-116.507	15	1940	2017	121	34	21	-2.1	664
Canada	Thetis Lake	TLPM	*Pseudotsuga menziesii* (Mirb.) Franco	48.462	-123.465	15	1928	2017	129	72	33	9.3	720
Czech Republic	Košetice	KSPA	*Picea abies* (L.) H.Karst.	49.566	15.091	15	1962	2017	75	45	29	7.8	626
Czech Republic	Soběšice	SOQP	*Quercus petraea* (Matt.) Liebl.	49.250	16.610	15	1984	2014	87	40	17	8.1	569
Germany	Garmisch	GAPA	*Picea abies* (L.) H.Karst.	47.494	11.065	15	1963	2017	97	51	36	3.1	1051
Germany	Niederhaverbek	NIPS	*Pinus sylvestris* L.	53.132	9.875	15	1984	2017	40	29	20	8.7	743
Germany	Tharandt	THPA	*Picea abies* (L.) H.Karst.	50.929	13.526	14	1997	2017	28	25	20	8.0	788
Hungary	Puspokszilagy	HCQC	*Quercus cerris* L.	47.752	19.302	15	1966	2017	77	34	NA	9.2	596
Hungary	Kerecsend	HEQP	*Quercus petraea* (Matt.) Liebl.	47.815	20.354	15	1977	2015	52	35	NA	9.8	583
Poland	Gleboki Brod	GBPS	*Pinus sylvestris* L.	53.950	23.210	14	1966	2017	73	40	31	6.9	564
Poland	Jaworzno	JAPS	*Pinus sylvestris* L.	50.194	19.315	15	1964	2017	82	30	22	8.2	731
Poland	Magdalenka	MAPS	*Pinus sylvestris* L.	52.080	20.941	15	1970	2017	62	36	22	8.2	542
Poland	Ostrow	OMPS	*Pinus sylvestris* L.	52.660	21.730	15	1960	2017	92	42	29	7.8	584
Poland	Rogów	ROQR	*Quercus robur* L.	51.806	19.911	15	1950	2016	86	42	29	8.1	585
Romania	Dumbravita	DBQR	*Quercus robur* L.	45.769	25.478	15	1903	2017	132	52	27	7.6	716
Romania	Reci	REPS	*Pinus sylvestris* L.	45.816	25.943	14	1959	2016	107	50	34	7.8	665
Russia	Raifa	RAPS	*Pinus sylvestris* L.	55.909	48.733	14	1900	1981	202	NA	20	3.9	527
Serbia	Avala	AVPN	*Pinus nigra* J.F.Arnold	44.672	20.541	12	1977	2017	49	34	20	12.0	642
Serbia	Deliblatski Pesak	DPPS	*Pinus sylvestris* L.	44.811	21.239	14	1976	2017	50	27	18	11.7	641
Serbia	Stepin Lug	SLPN	*Pinus nigra* J.F.Arnold	44.748	20.531	15	1976	2017	53	28	18	12.0	642
Switzerland	Albisboden	ABPA	*Picea abies* (L.) H.Karst.	47.269	8.525	15	1990	2017	37	43	27	8.3	1435
United Kingdom	North England	UKPA	*Picea abies* (L.) H.Karst.	54.000	-2.400	14	1998	2017	25	18	14	8.6	1273

Table 1: Meta data summary for all sites and species included in the study. Sites are sorted by country. Latitude and longitude in decimal degrees. N: Number of trees for which an eastern and a southern core was sampled; 1st yr, Last yr: First and last year of the common overlap period shared by all ring-width series of a site; M.s.length: Mean series length in years (calculated across eastern and southern cores); M.DBH: Mean diameter at breast height in cm; M.height: Mean tree height in m. Temp: Mean annual temperature in °C; Prec: Mean yearly precipitation sums in mm.

Appendix A: Supplementary online material

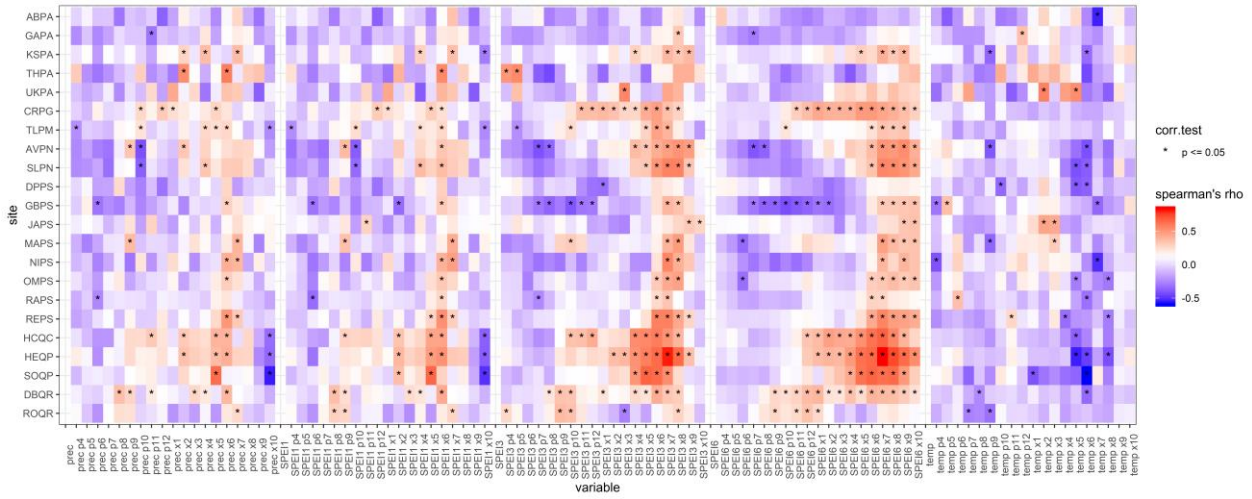

Fig. A1: Heatmap of coefficients calculated for correlations between climate variables and site master chronologies. Sites are sorted by species. For abbreviations see article.

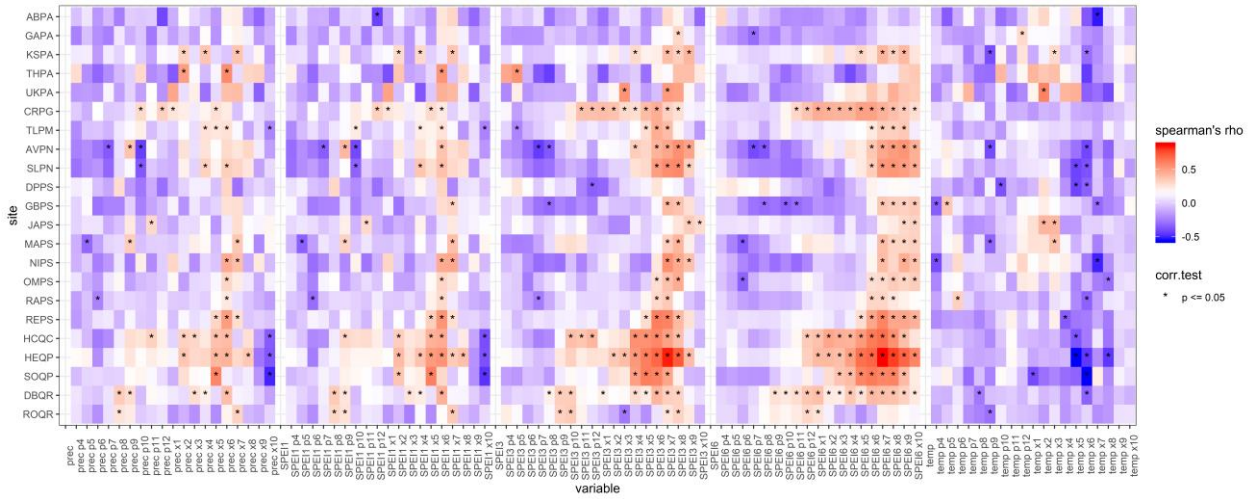

Fig. A2: Heatmap of coefficients calculated for correlations between climate variables and eastern core chronologies. Sites are sorted by species. For abbreviations see article.

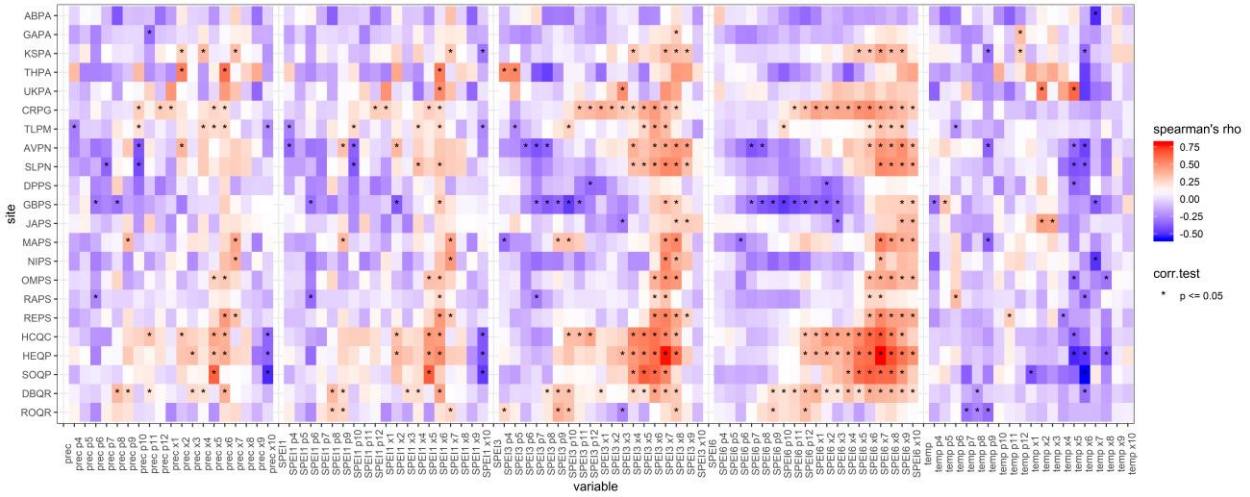

Fig. A3: Heatmap of coefficients calculated for correlations between climate variables and southern core chronologies. Sites are sorted by species. For abbreviations see article.

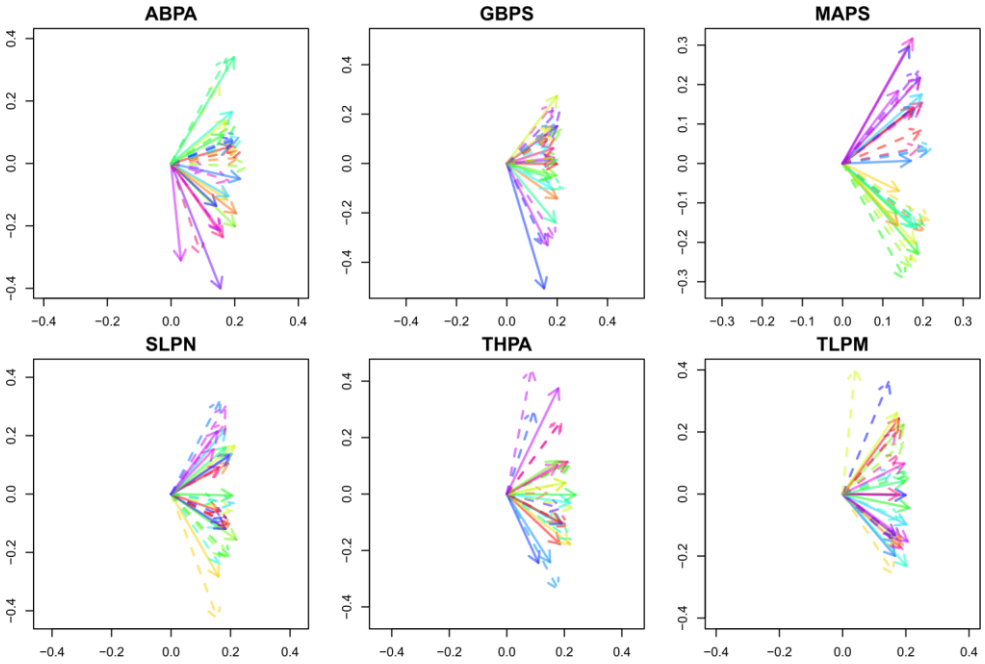

Fig. A4: Examples for visualizing the Wilcoxon Signed-Rank test (p-values on Fig. 4). One color per individual tree with eastern cores as dashed arrows and southern cores as solid arrows. Ratio of variance explained by PC1 and PC2 as on Fig. 4 in article.